

Origin of Spin Ice Behavior in Ising Pyrochlore Magnets with Long Range Dipole Interactions: an Insight from Mean-Field Theory

Michel J.P. Gingras^{1,2} and Byron C. den Hertog¹

¹*Department of Physics, University of Waterloo, Ontario Canada N2L 3G1*

²*Canadian Institute for Advanced Research, 180 Dundas Street West, Toronto, Ontario, M5G 1Z8, Canada*
(November 3, 2018)

Recent experiments suggest that the Ising pyrochlore magnets $\text{Ho}_2\text{Ti}_2\text{O}_7$ and $\text{Dy}_2\text{Ti}_2\text{O}_7$ display qualitative properties of the ferromagnetic nearest neighbor spin ice model proposed by Harris *et al.*, Phys. Rev. Lett. **79**, 2554 (1997). The manifestation of spin ice behavior in these systems *despite* the energetic constraints introduced by the strength and the long range nature of dipole-dipole interactions, remains difficult to understand. We report here results from a mean field analysis that shed some light on the origin of spin ice behavior in (111) Ising pyrochlores. Specifically, we find that there exist a large frustrating effect of the dipolar interactions beyond the nearest neighbor, and that the degeneracy established by effective ferromagnetic nearest neighbor interactions is only very weakly lifted by the long range interactions. Such behavior only appears beyond a cut-off distance corresponding to $O(10^2)$ nearest neighbor. Our mean field analysis shows that truncation of dipolar interactions leads to spurious ordering phenomena that change with the truncation cut-off distance.

To appear in Canadian Journal of Physics for the Proceedings of the *Highly Frustrated Magnetism 2000 Conference*, Waterloo, Ontario, Canada, June 11-15, 2000

PACS numbers: 75.50.Ee, 75.40.Cx, 75.30.Kz, 75.10.-b,

I. INTRODUCTION

The past five years have seen a resurgence of significant interest devoted to the systematic study of geometrically frustrated magnetic systems [1–5]. Frustration arises when a magnetic system cannot minimize its total classical ground-state energy by minimizing the energy of each spin-spin interaction individually [6]. This most often occurs in materials containing antiferromagnetically coupled magnetic moments that reside on geometrical units, such as triangles and tetrahedra, which inhibit the formation of a collinear magnetically-ordered state.

It is very common for models of highly frustrated magnetic systems to display ground state degeneracies where the system is “underconstrained”, giving many distinct spin configurations give the same ground state energy. The best known example is probably that of the two-dimensional Ising antiferromagnet on a simple triangular lattice, for which it was shown by Wannier that the ground state is macroscopically degenerate with an extensive ground state entropy [7]. Another example is the nearest-neighbor antiferromagnet face-centered cubic lattice with Heisenberg [8–12], and Ising spins [13]. In the past ten years, much attention has been devoted to the kagomé lattice of corner-sharing triangles, and the pyrochlore lattice of corner-sharing tetrahedra with Heisenberg spins interacting via nearest neighbor antiferromagnetic interactions [1–5].

Typically, there are two generic class of mechanisms that can lift the degeneracies in frustrated magnetic systems. The most common and simplest mechanism proceeds via energetic perturbations beyond the term(s) in the spin Hamiltonian that cause the degeneracies. Degeneracies can also be lifted by either thermal fluctuations or quantum zero-point fluctuations [3,4,14–19].

There are a number of well known situations where spin interactions beyond nearest neighbor cause long range order that would otherwise be absent in a highly frustrated lattice with only nearest neighbor antiferromagnetic exchange present. For example, the classical kagomé [20] and pyrochlore [16,17,21] nearest neighbor Heisenberg antiferromagnet lattices display either Néel order or a dramatic reduction of ground state degeneracy when exchange interactions beyond nearest neighbor are considered. Long range dipole-dipole interactions in the FCC Heisenberg antiferromagnet [11,12] and in the pyrochlore lattice with Heisenberg spins (as pertains to the $\text{Gd}_2\text{Ti}_2\text{O}_7$ pyrochlore material [22–24]), have also been shown to reduce significantly the degeneracy otherwise present in the nearest neighbor version of these systems.

While high geometric frustration usually arises in antiferromagnetic systems, Harris and collaborators recently showed that the pyrochlore lattice of corner sharing tetrahedra with Ising spins pointing along a local cubic (111) axis (See Fig. 1) constitutes an interesting and unusual example of high geometric frustration when the nearest neighbor interaction is actually ferromagnetic [25,26]. Harris and collaborators introduced the concept of *spin ice* to emphasize the analogy between ferromagnetically coupled (111) Ising moments on the pyrochlore lattice and the problem of proton ordering in common hexagonal ice, I_h [25–28]. In the simple model of nearest neighbor ferromagnetic interactions, the system has the same ‘ice rules’ for the construction of its ground state as those for the ground state of real ice [29], hence the name *spin ice*. The resulting extensive ground state entropy of hexagonal ice was first estimated by Pauling in 1935 [30] which, remarkably, provides a fairly accurate estimate of the residual low temperature entropy of real pyrochlore spin ice materials [31].

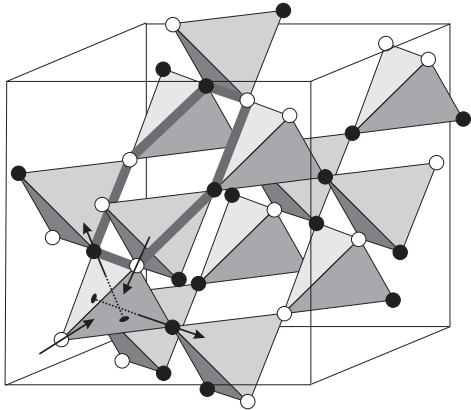


FIG. 1. The lower left ‘downward’ tetrahedron of the pyrochlore lattice shows Ising spins (arrows). Each spin axis is along the local (111) quantization axis, which goes from one site to the middle of the opposing triangular face (as shown by the disks on the triangular faces) and meets with the three other (111) axes in the middle of the tetrahedron. For clarity, black and white circles on the lattice points denote other spins. White represents a spin pointing into a downward tetrahedron while black is the opposite. The entire lattice is shown in an ice-rules state (two black and two white sites for every tetrahedron). The hexagon (thick gray line) shows a low energy “loop” excitation (see text) which corresponds to reversing all colors (spins) on the loop to produce a new ice-rules state.

Interestingly, materials with local (111) Ising spins are realized in $\text{Ho}_2\text{Ti}_2\text{O}_7$ [25,32–34], $\text{Dy}_2\text{Ti}_2\text{O}_7$ [31] and $\text{Tb}_2\text{Ti}_2\text{O}_7$ [35–38], where the rare earth magnetic moments (Ho^{3+} , Dy^{3+} and Tb^{3+}) reside on the sites of the pyrochlore lattice. For (111) Ising pyrochlore systems, each moment points along the axis joining the centers of the two tetrahedra that it belongs to (see Fig. 1). For ferromagnetic nearest neighbor interaction, the ground state is macroscopically degenerate, but with the constraint that two moments must point in and two must point out of every tetrahedron which, as mentioned above, is a constraint that maps precisely onto the ice rules [25–30].

The nearest neighbor model of Harris and Bramwell [26] shows no evidence of a magnetic transition to long range magnetic order [27,28,39], but displays a broad peak in the specific heat at a temperature of the order of the nearest neighbor ferromagnetic coupling. Both $\text{Ho}_2\text{Ti}_2\text{O}_7$ [25,32–34] and $\text{Dy}_2\text{Ti}_2\text{O}_7$ [31] show qualitative behavior consistent with this spin ice picture.

As explained above, the occurrence of a macroscopic degeneracy in frustrated magnetic is due to “underconstraints”; many different spin configurations (here the ice-rules “two-in–two-out” per tetrahedron) give the same ground state energy. We therefore expect that the microscopic origin of the spin ice phenomenon in $\text{Ho}_2\text{Ti}_2\text{O}_7$ and $\text{Dy}_2\text{Ti}_2\text{O}_7$ has to directly involve such a manifestation of underconstraints in the energetics involved in the formation of the spin ice ground state.

Our goal is therefore to understand how the competing energy scales in the spin ice materials are able to produce underconstraints. In order to identify such underconstraints, we must first consider the various energy scales at play in the above materials. Firstly, the single-ion ground state for Ho^{3+} and Dy^{3+} in the pyrochlore structure is well described by an effective classical Ising doublet with a ground state magnetic moment of $\mu \approx 10\mu_B$ and a nearest neighbor distance, r_{nn} , of approximately 3.54\AA for both materials [33]. For two nearest neighbor moments pointing along their local (111) direction, the nearest neighbor dipole-dipole energy scale, D_{nn} , is

$$D_{nn} = \frac{5}{3} \left(\frac{\mu_0}{4\pi} \right) \frac{\mu^2}{r_{nn}^3} \approx +2.35\text{K} \quad , \quad (1.1)$$

where, as discussed in the next section, the $5/3$ factor comes from the orientation of the Ising quantization axes relative to the vector direction connecting interacting nearest neighbor magnetic moments. Interestingly, D_{nn} is positive (i.e. ferromagnetic) and therefore, as in the Harris and Bramwell nearest neighbor model [26], is frustrating for Ising spins on a tetrahedron.

The experimentally determined Curie-Weiss temperature, θ_{CW} , extrapolated from temperatures below $T \sim 100\text{K}$ is $+1.9\text{K}$ for $\text{Ho}_2\text{Ti}_2\text{O}_7$ [25] and $+0.5\text{K}$ for $\text{Dy}_2\text{Ti}_2\text{O}_7$ [31], respectively. These two values show that θ_{CW} is of the same order of magnitude as the nearest neighbor dipolar energy scale. Furthermore, it is well known that rare-earth ions possess very small exchange energies. Consequently, dipole-dipole interactions in $\text{Ho}_2\text{Ti}_2\text{O}_7$ and $\text{Dy}_2\text{Ti}_2\text{O}_7$ constitute a preponderant interaction, as opposed to a weak perturbation as in magnetic transition elements where the exchange interaction predominates over dipolar interactions. As we discuss below, fits to experimental data show that the nearest neighbor exchange interaction is antiferromagnetic for both $\text{Ho}_2\text{Ti}_2\text{O}_7$ and for $\text{Dy}_2\text{Ti}_2\text{O}_7$ and, when considered alone, is therefore not frustrating for (111) Ising moments on the pyrochlore lattice [18,26,40]. In order to consider the combined role of exchange and dipole-dipole interactions, we find it useful to define an effective nearest neighbor energy scale, J_{eff} , for (111) Ising spins:

$$J_{\text{eff}} \equiv J_{nn} + D_{nn} \quad , \quad (1.2)$$

where J_{nn} is the nearest neighbor exchange energy between (111) Ising moments. This simple description predicts that a (111) Ising system would display spin ice properties even for antiferromagnetic nearest neighbor exchange, $J_{nn} < 0$, but has long as $J_{\text{eff}} = J_{nn} + D_{nn} > 0$. Fits to experimental data give $J_{nn} \sim -0.52\text{K}$ for $\text{Ho}_2\text{Ti}_2\text{O}_7$ [34] and $J_{nn} \sim -1.24\text{K}$ for $\text{Dy}_2\text{Ti}_2\text{O}_7$ [41]. Thus, J_{eff} is positive (using $D_{nn} = 2.35\text{K}$) hence ferromagnetic and frustrated for both $\text{Ho}_2\text{Ti}_2\text{O}_7$ and $\text{Dy}_2\text{Ti}_2\text{O}_7$, but not for $\text{Tb}_2\text{Ti}_2\text{O}_7$ for which $J_{nn} \approx -0.9\text{K}$ and $D_{nn} = +0.8\text{K}$ [35–38]. It would therefore appear natural to ascribe the spin ice behavior in both $\text{Ho}_2\text{Ti}_2\text{O}_7$ and $\text{Dy}_2\text{Ti}_2\text{O}_7$ to the positive J_{eff} value as in the simple model of Harris and Bramwell [25,26]. However, the situation is much more complex than it naively appears, especially when considering the spin ice phenomenon in the context of an underconstrained problem.

The main conceptual difficulty in intuitively understanding the physical origin of spin ice behavior in rare-earth titanates stems from the very nature of the large dipole-dipole interactions in the $\text{Dy}_2\text{Ti}_2\text{O}_7$ and $\text{Ho}_2\text{Ti}_2\text{O}_7$ materials. Recall the general discussion above on the role of perturbations in frustrated magnetic systems with degenerate ground states. Dipole-dipole interactions are “complicated” in that (i) they are strongly anisotropic since they couple the spin, $\mathbf{S}_i^{\hat{z}_i}$, and space, \mathbf{r}_{ij} , directions, and (ii) they are also very long range ($\propto 1/r_{ij}^3$). One would naively expect that both the spin-space coupling, $(\mathbf{S}_i^{\hat{z}_i} \cdot \mathbf{r}_{ij})$, and the long range nature of the interaction (beyond nearest neighbor) introduces “so many” energetic constraints on the ground state spin correlations that consideration of the dipolar interaction beyond nearest neighbor would lift most, if not all local degeneracies. Such an effect would give rise to a long range ordered state at a well defined (possibly incommensurate) wave vector at some critical temperature $T_c(J, D) \sim O(D_{\text{nn}}/k_B) \sim 2$ K, as opposed to spin ice behavior. This simple argument would appear to be further supported by noting that recent calculations show that vanishingly small, but nonzero long range dipole-dipole interactions select a unique (non-degenerate) long range Néel ordered state for Heisenberg spins in an otherwise classical nearest neighbor pyrochlore antiferromagnet [22,23]. This clearly does not happen in real spin ice materials such as $\text{Ho}_2\text{Ti}_2\text{O}_7$ [25,34] and $\text{Dy}_2\text{Ti}_2\text{O}_7$ [31], at least down to a temperature $T \sim 200$ mK. Hence the question that we address here is:

When there is an effective ferromagnetic nearest neighbor interaction, J_{eff} , in (111) Ising pyrochlores, why do long range dipolar interactions fail to destroy spin ice behavior, and not, instead, give rise to long range Néel order with a critical temperature $T_c \sim O(D_{\text{nn}})$?

A simple explanation to this question might be that the inability of long range dipolar interactions to lift the ground state degeneracy established at the nearest neighbor level arises from a “mutual frustration” of the degeneracy-lifting energetics, or mean-field, coming from the spins beyond the nearest neighbor distance. This argumentation, if correct, suggests that a mean-field theory which contains dipolar interactions up to an “appropriate cut off” distance, and aimed at determining the ordering wave vector as a function of the cut-off distance of the dipolar interactions may be used as a first step to investigate the microscopic origin of spin ice behavior, and the failure of a dipolar-driven degeneracy lifting process at a temperature $T \sim O(D_{\text{nn}})$. As we show below, we find that the truncation of dipolar interactions lead to spurious results when the truncation distance is less than $\lesssim 100$ nearest neighbors, and that spin ice behavior is restored only when considering the dipolar interactions to very large cut-off distances.

The rest of the paper is organized as follows. In the next section we present a description of the mean-field theory we use to determine the ordering wavevector in (111) Ising pyrochlores as a function of cut-off distance. Our results are presented in Section III, followed by a

brief discussion in Section IV.

II. MEAN-FIELD THEORY

Our aim in this section is to use mean-field theory to determine the the critical (“soft”) modes and, consequently, the nature of the magnetic phase(s) exhibited by a classical model of Ising spins on a pyrochlore lattice with local axes (the (111) directions of the cubic unit cell). This system is described by a Hamiltonian with nearest neighbor exchange and long range dipolar interactions [41,42]:

$$H = -J \sum_{\langle ij \rangle} \mathbf{S}_i^{\hat{z}_i} \cdot \hat{\mathbf{S}}_j^{\hat{z}_j} + D r_{\text{nn}}^3 \sum_{i>j} \frac{\mathbf{S}_i^{\hat{z}_i} \cdot \mathbf{S}_j^{\hat{z}_j}}{|\mathbf{r}_{ij}|^3} - \frac{3(\mathbf{S}_i^{\hat{z}_i} \cdot \mathbf{r}_{ij})(\mathbf{S}_j^{\hat{z}_j} \cdot \mathbf{r}_{ij})}{|\mathbf{r}_{ij}|^5} . \quad (2.1)$$

The first term is the near neighbor exchange interaction, and the second term is the dipolar coupling between the (111) Ising magnetic moments. For the open pyrochlore lattice structure, we expect very small second and further nearest neighbor exchange coupling [43]. We therefore only consider exchange interactions between nearest neighbor spins. Here the spin vector $\mathbf{S}_i^{\hat{z}_i}$ labels the Ising moment of magnitude $|\mathbf{S}_i^{\hat{z}_i}| = 1$ at lattice site i and oriented along the *local* Ising (111) axis \hat{z}_i . The distance $|\mathbf{r}_{ij}|$ is measured in units of the nearest neighbor distance, r_{nn} . Here J represents the exchange energy and $D = (\mu_0/4\pi)\mu^2/r_{\text{nn}}^3$. Because of the local Ising axes, the effective nearest neighbor energy scales are $J_{\text{nn}} \equiv J/3$ and, as mentioned above, $D_{\text{nn}} \equiv 5D/3$, since $\hat{z}_i \cdot \hat{z}_j = -1/3$ and $(\hat{z}_i \cdot \mathbf{r}_{ij})(\mathbf{r}_{ij} \cdot \hat{z}_j) = -2/3$.

We now proceed along the lines of Reimers, Berlinsky and Shi in their mean-field study of Heisenberg pyrochlore antiferromagnets [21], and which has recently been extended to investigate systems with long range dipole-dipole interactions [22,23]. We consider the mean-field order parameters, $\mathbf{B}(\mathbf{r}_i)$ at site \mathbf{r}_i . The pyrochlore lattice is a non-Bravais lattice, and we use a rhombohedral basis where there are four atoms per unit cell located at $(0, 0, 0)$, $(1/4, 1/4, 0)$, $(1/4, 0, 1/4)$, and $(0, 1/4, 1/4)$ in units of the conventional cubic unit cell of size $a = r_{\text{nn}}\sqrt{8}$. Each of these four points define an FCC sublattice of cubic unit cell of size a . We relabel the spins, $\mathbf{S}(\mathbf{r}_i)$, in terms of unit cell coordinates, and a sublattice index within the unit cell, and take advantage of the translational symmetry of the lattice by expanding the order parameters $\mathbf{B}(\mathbf{r}_i)$ in terms of Fourier components. In this case $\mathbf{B}^a(\mathbf{r}_i) = B(\mathbf{r}_i)\hat{z}_i^a$ on the a 'th sublattice site of the unit cell located at \mathbf{r}_i can be written as

$$B^a(\mathbf{r}_i)\hat{z}_i^a = \sum_{\mathbf{q}} B^a(\mathbf{q})\hat{z}_i^a \exp(i\mathbf{q} \cdot \mathbf{r}_i) , \quad (2.2)$$

where \hat{z}_i^a is a unit vector along the local $\langle 111 \rangle$ Ising axis on the i 'th site of sublattice a . The spin-spin interaction matrix, $\mathcal{J}^{ab}(|\mathbf{r}_{ij}|)$, including both exchange and dipolar interactions, reads:

$$\mathcal{J}^{ab}(|\mathbf{r}_{ij}|) = J(\hat{z}_i^a \cdot \hat{z}_j^b) \delta_{r_{ij}, r_{\text{nn}}} \quad (2.3)$$

$$+ D_{dd} \left\{ \frac{\hat{z}_i^a \cdot \hat{z}_j^b}{(r_{ij}^{ab})^3} - 3 \frac{\hat{z}_i^a \cdot \mathbf{r}_{ij}^{ab} \hat{z}_j^b \cdot \mathbf{r}_{ij}^{ab}}{(r_{ij}^{ab})^5} \right\}, \quad (2.4)$$

where $\delta_{\alpha\beta}$ is the Kronecker delta. \mathbf{r}_{ij}^{ab} denotes the inter-spin vector \mathbf{r}_{ij} that connects spin \mathbf{S}_i^a on the a sublattice to spin \mathbf{S}_j^b on the b sublattice. We write $\mathcal{J}^{ab}(|\mathbf{r}_{ij}|)$ in terms of its Fourier components as

$$\mathcal{J}^{ab}(|\mathbf{r}_{ij}|) = \frac{1}{M_{\text{cell}}} \sum_{\mathbf{q}} \mathcal{J}^{ab}(\mathbf{q}) \exp(-i\mathbf{q} \cdot \mathbf{r}_{ij}) \quad (2.5)$$

where M_{cell} is the number of unit cells with 4 spins per unit cell. The quadratic part of the mean-field free-energy, $F^{(2)}$, then becomes [21]:

$$F^{(2)}(T)/M_{\text{cell}} = \frac{1}{2} \sum_{\mathbf{q}, (ab)} B^a(\mathbf{q}) \{T\delta_{ab} - \mathcal{J}^{ab}(\mathbf{q})\} B^b(-\mathbf{q}), \quad (2.6)$$

where T is the temperature in units of $1/k_B$. Diagonalizing $F^{(2)}(T)$ requires transforming to normal modes of the system

$$B^a(\mathbf{q}) = \sum_{\alpha} U^{a,\alpha} \Phi^{\alpha}(\mathbf{q}), \quad (2.7)$$

where $\{\Phi^{\alpha}(\mathbf{q})\}$ are the eigenmodes, and $U(\mathbf{q})$ is the unitary matrix that diagonalizes $\mathcal{J}^{ab}(\mathbf{q})$ in the sublattice space, with eigenvalues $\lambda^{\alpha}(\mathbf{q})$

$$\sum_b \mathcal{J}^{ab}(\mathbf{q}) U^{b\alpha}(\mathbf{q}) = \lambda^{\alpha}(\mathbf{q}) U^{a\alpha}(\mathbf{q}). \quad (2.8)$$

Henceforth we use the convention that indices (ab) label sublattices, and index α labels the normal modes. We express $F^{(2)}(T)$ in terms of normal modes as

$$F^{(2)}/M_{\text{cell}} = \frac{1}{2} \sum_{\mathbf{q}} \sum_{\alpha} \Phi^{\alpha}(\mathbf{q}) \Phi^{\alpha}(-\mathbf{q}) \{k_B T - \lambda^{\alpha}(\mathbf{q})\}. \quad (2.9)$$

An ordered state first occurs at the temperature

$$T_c = \max_{\mathbf{q}} \{\lambda^{\max}(\mathbf{q})\}, \quad (2.10)$$

where $\lambda^{\max}(\mathbf{q})$ is the largest of the four eigenvalues ($\alpha = 1, 2, 3, 4$) at wavevector \mathbf{q} , and where $\max_{\mathbf{q}}$ indicates a global maximum of the spectrum of $\lambda^{\max}(\mathbf{q})$ for all \mathbf{q} . The value of \mathbf{q} for which $\lambda^{\alpha}(\mathbf{q})$ is maximum is the ordering wavevector \mathbf{q}_{ord} .

Let us briefly explain how we proceed using the above set of equations to determine the critical (“soft”) mode(s) of the system at T_c . The Fourier transform of $\mathcal{J}^{ab}(|\mathbf{r}_{ij}|)$ is calculated using the inverse transform of Eq. (2.5). The pyrochlore lattice has a symmetry of inversion with respect to a lattice point and this implies that $\mathcal{J}^{ab}(\mathbf{q})$ is real and symmetric. The eigenvalues and eigenvectors are found using a standard numerical packages for eigen problems of real symmetric matrices.

III. RESULTS

For each \mathbf{q} there are 4 eigenvalues of $\mathcal{J}^{ab}(\mathbf{q})$ ($\lambda^{\alpha}(\mathbf{q})$, $\alpha = 1, 2, 3, 4$). To determine \mathbf{q}_{ord} we need to find the \mathbf{q} value for which λ^{α} is maximum. We therefore calculate $\lambda^{\max}(\mathbf{q})$, the largest of the 4 eigenvalues of $\mathcal{J}^{ab}(\mathbf{q})$ for each \mathbf{q} . Figures 2–6 show $\lambda^{\max}(\mathbf{q})$ vs \mathbf{q} in the (hhl) plane for various cut-off distance, N_c , of the dipolar interactions used in the calculation of $\mathcal{J}^{ab}(\mathbf{q})$ via the inverse transform of Eq. 2.5. Figures 2–6 correspond to cut-off distances for the 1st, 2nd, 5th, 100th and 1000th nearest neighbor ($N_c = 1, 2, 5, 100$ and 1000), and which correspond to physical distances $R_c(N_c = 1)/r_{\text{nn}} = 1$, $R_c(N_c = 5)/r_{\text{nn}} = \sqrt{7}$, $R_c(N_c = 10)/r_{\text{nn}} = \sqrt{13}$, $R_c(N_c = 100)/r_{\text{nn}} = \sqrt{136}$ and $R_c(N_c = 1000)/r_{\text{nn}} = 37$, expressed in units of the nearest neighbor distance, r_{nn} . In the calculations here, we have used $J = 0$ and measure $\lambda^{\max}(\mathbf{q})$ in units of the dipolar strength, D . Our conclusions below are independent of the choice made for J as long as we are in the spin-ice regime ($J/3 + 5D/3 \gtrsim 0$). For J sufficiently negative (antiferromagnetic) the ordering wavevector is at $\mathbf{q}_{\text{ord}} = 0$, corresponding to a two-fold Ising state all-in–all-out as discussed in Refs. [18,26,40,41]. Several comments are in order.

Cutting off the dipolar interaction at $N_c = 1$ gives the effective nearest neighbor Hamiltonian:

$$H_{\text{eff}}(N_c = 1) = \left(\frac{J}{3} + \frac{5D}{3} \right) \sum_{\langle i,j \rangle} \sigma_i \sigma_j, \quad (3.1)$$

where $\sigma_i = \pm 1$. For $J_{\text{eff}} = (J + 5D)/3 = J_{\text{nn}} + D_{\text{nn}} > 0$, and we recover the nearest neighbor Ising spin ice model of Harris and Bramwell [25,26]. As discussed in Refs. [25,26], this model maps onto Anderson’s antiferromagnetic Ising model with global \hat{z} quantization axis [28]. Consequently, it is normal to recover in Fig. 2 the spectrum of $\lambda^{\max}(\mathbf{q})$ found for the pyrochlore antiferromagnet [21]. Indeed, the largest eigenvalue found in Ref. [21] is $2J_{\text{eff}}$. Using $J_{\text{eff}} = J_{\text{nn}} + D_{\text{nn}} = 5D/3$, we get the flat spectrum at $\lambda(\mathbf{q})/D = 10/3$, as in Fig. 2. (In Figs. 2-7, \mathbf{q} is measured in units of $2\pi/a$). The flatness of $\lambda^{\max}(\mathbf{q})$ reflects the \mathbf{q} -space representation of the zero energy excitation modes in real space. In the kagomé Heisenberg antiferromagnet lattice, these are the so-called weather-vane modes [2,14]. Here, for Ising spins, they correspond to closed loops of equal in and out spins which obey the ice-rules [28–30]. These were first identified by Anderson [28], and have recently been exploited in computer simulations of the dipolar spin ice model [42].

In Fig. 3 we see that $\lambda^{\max}(\mathbf{q})$ develops an absolute maximum for $N_c = 5$. This means that a well defined mode becomes soft (massless) at the corresponding incommensurate \mathbf{q}_{ord} , which should give rise to incommensurate long range Néel order, unlike what was found in Refs. [32,44] for their choice $N_c = 5$. We comment on this further in Section IV.

For $N_c = 10$ (Fig. 4), we see that \mathbf{q}_{ord} is different from its value for $N_c = 5$. Clearly, \mathbf{q}_{ord} is not a rapidly converging function of N_c . We note also that some of the flatness present for $N_c = 1$ shown in Fig. 2 is being recovered for $N_c = 10$. For $N_c = 100$ (Fig. 5), we

clearly note modulations (“ripples”) in $\lambda^{max}(\mathbf{q})$ in the $\langle 111 \rangle$ direction, with now increased flatness restored in the overall spectrum. As N_c is increased, these modulations “interfere” in such a manner as to restore a very smooth surface, as shown in Fig. 6 for $N_c = 1000$. This is similar to what is found in the classical Heisenberg pyrochlore lattice with long range dipole-dipole interactions where the amplitude of the ripples in the $\langle 111 \rangle$ directions are continuously decreasing and mutually cancelling out each other as the number of nearest neighbor distances considered in the dipolar lattice sum is increased to infinity and where, in the limit $N_c \rightarrow \infty$, a degeneracy line occurs at the star of $\langle 111 \rangle$ [22,23]. Essentially, the ripples get smoothed out and pushed to zero as the finite-size effect of the cut-off wavevector $q_c \sim 2\pi/R_c(N_c)$ goes to zero. This is more explicitly shown in Fig. 7 where $\lambda^{max}(hh0)$ is shown. The convergence at strictly $\mathbf{q} = 0$ is slow since the dipolar lattice sum is conditionally convergent for this \mathbf{q} value. This is the origin of the downward “spike” in Fig. 7 for $\mathbf{q} = 0$.

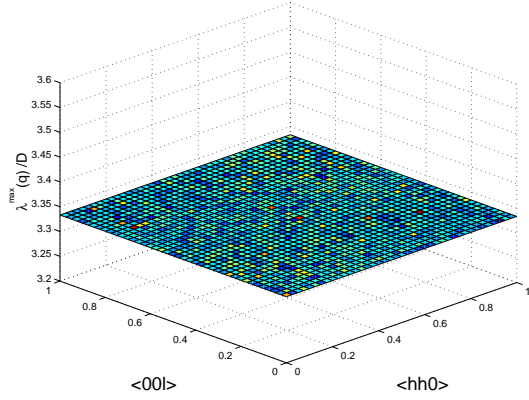


FIG. 2. $\lambda^{max}(\mathbf{q})$ vs \mathbf{q} in the $\langle hhl \rangle$ plane for $N_c = 1$.

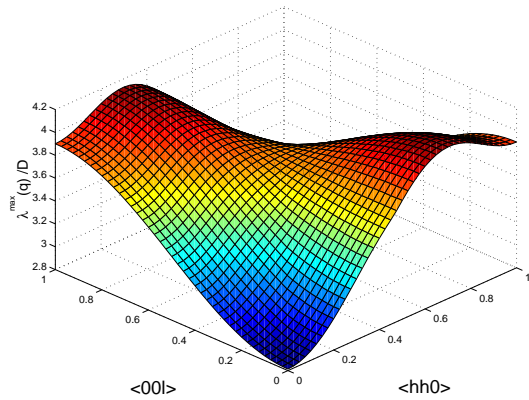


FIG. 3. $\lambda^{max}(\mathbf{q})$ vs \mathbf{q} in the $\langle hhl \rangle$ plane for $N_c = 5$.

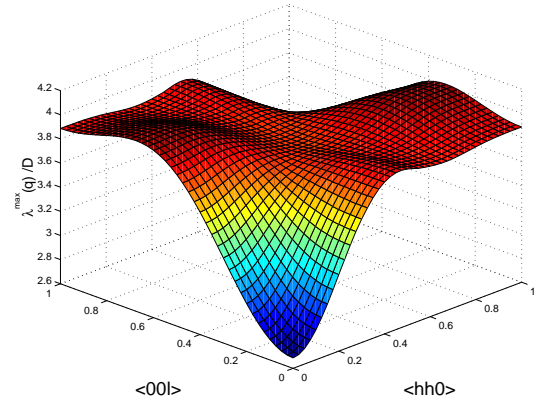


FIG. 4. $\lambda^{max}(\mathbf{q})$ vs \mathbf{q} in the $\langle hhl \rangle$ plane for $N_c = 10$.

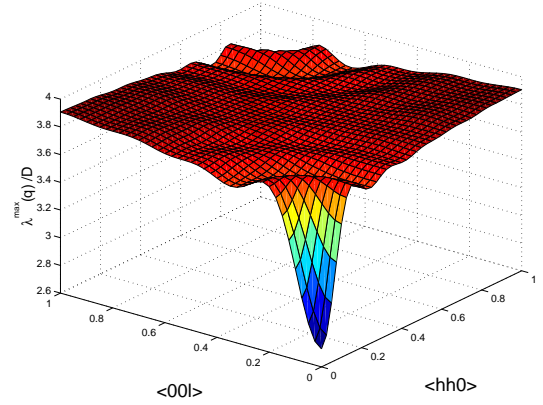


FIG. 5. $\lambda^{max}(\mathbf{q})$ vs \mathbf{q} in the $\langle hhl \rangle$ plane for $N_c = 100$.

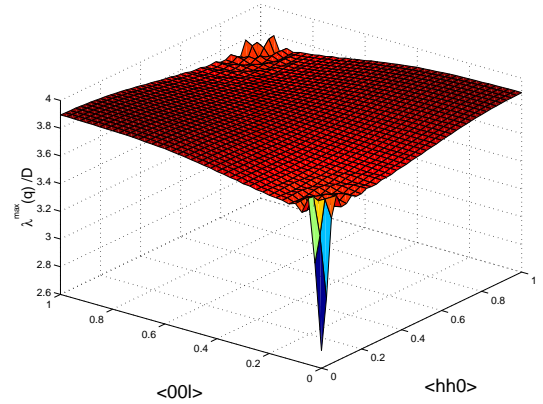


FIG. 6. $\lambda^{max}(\mathbf{q})$ vs \mathbf{q} in the $\langle hhl \rangle$ plane for $N_c = 1000$.

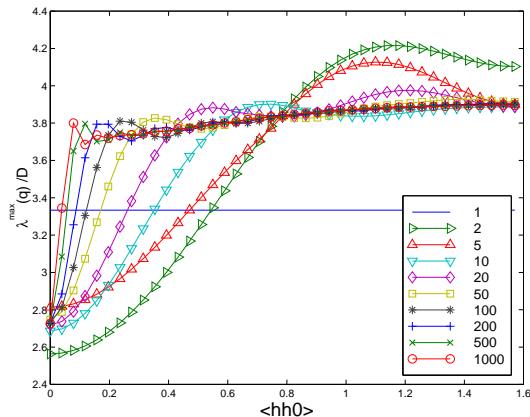


FIG. 7. $\lambda^{max}(\mathbf{q})$ vs \mathbf{q} for \mathbf{q} in the $\langle 100 \rangle$ direction, for $N_c = 1$ (solid line, no symbols), $N_c = 2$ (right triangles), $N_c = 5$ (up triangles), $N_c = 10$ (down triangles), $N_c = 20$ (diamond), $N_c = 50$ (squares), $N_c = 100$ (stars), $N_c = 200$ (pluses), $N_c = 500$ (crosses), and $N_c = 1000$ (circles).

IV. DISCUSSION

Figure 6 constitutes our main result. We see that as $N_c \rightarrow \infty$, the spectrum of $\lambda^{max}(\mathbf{q})$ becomes very flat, similar but not identical to the nearest neighbor spin ice model (Fig. 2). This shows that it is the very long distance behavior of dipolar interactions leads to a high frustration that restores the symmetry and loops as low-energy excitations obeying the ice-rules [28,42], and, therefore, causes the spin ice phenomenon in Ising pyrochlore rare-earths systems. One notes that $\lambda^{max}(\mathbf{q})$ displays a weak maximum at $\mathbf{q}_{ord} = (2\pi/a)[1, 0, 0]$. The low-lying maximum and weak dispersion of $\lambda^{max}(\mathbf{q})$ when $N_c \rightarrow \infty$ with respect to the overall smooth and flat profile of the spectrum implies a small ordering temperature, T_c , compared to the nearest neighbor dipolar energy scale, D , in agreement with our recent loop Monte Carlo simulations where we found $T_c/D \sim 0.11$ [42]. Also, \mathbf{q}_{ord} found here in the mean-field theory for $N_c \rightarrow \infty$ is the same ordering wave vector as the one found in our Monte Carlo simulations [42]. Consequently, the answer to the question raised in the Introduction does appear to be that there is indeed a high level of frustration in spin ice materials that come from the energetics beyond nearest-neighbor. However, this frustration is not perfect, and there is indeed a lifting of the degeneracy caused by the dipoles, but only at a temperature scale $T/D \sim 0.1$.

The results presented here of the quasi-degeneracy in $\lambda^{max}(\mathbf{q})$, and the consequential spin ice behavior being recovered when $N_c \rightarrow \infty$ (as found in our Monte Carlo simulations [41,42] also), raise some questions as to the validity of the simulation work of Refs. [32] and [44] where dipole-dipole interactions were cut-off for $N_c = 5$ [32] and $N_c = 12$ [44]. We believe that the results of Refs. [32] and [44] are invalid as pertaining to real materials due to the truncation used for the dipolar sum. Specifically, for the values used in Ref. [32] to model $\text{Ho}_2\text{Ti}_2\text{O}_7$, and with a choice of $N_c = 5$, we have found in Monte Carlo simulations that the paramagnetic scattering is indeed

incommensurate [45], in agreement with our mean-field calculations. The constraint to work with a small number of unit cells and system size L incompatible with an incommensurate \mathbf{q}_{ord} that would be selected for $N_c = 5$ for a thermodynamically large sample may precipitate the system into a partially ordered state via some type of freezing transition as found in Ref. [32]. Conceptually, this is similar to the difficulties in finding the appropriate long range ordered vortex lattice ground state in Monte Carlo simulations of dense frustrated Josephson junction arrays in a magnetic field, and where glassy behavior is found when too small system sizes are considered [46,47]. At any rate, what happens in a simulation with $N_c \lesssim O(10^2)$ nearest neighbors is a moot issue in terms of modeling and understanding spin ice in real materials as our analysis here shows.

In conclusion, we have shown that one can understand at the mean-field level that it is the true long range nature of dipolar interactions that cause the quasi-degenerate ice-rules obeying states in Ising pyrochlore magnets such as $\text{Ho}_2\text{Ti}_2\text{O}_7$ and $\text{Dy}_2\text{Ti}_2\text{O}_7$. However, similar to the so-called energetic ice models [48,49], dipolar interactions do slightly energetically select a preferred state with long range Néel order at very low temperature. It would be interesting and useful to understand what is the specific relationship between the symmetry of long range dipolar interactions for local (111) Ising spins coupled via long range dipolar interactions, and the symmetry of the pyrochlore lattice that leads to an asymptotic restoration of a approximately ice-rules obeying quasi-degenerate ground state manifold.

ACKNOWLEDGMENTS

We thank Steve Bramwell and Peter Holdsworth for stimulating discussions. We acknowledge Maxime Dion and Roger Melko for collaborations on these and related studies. This reserach has been funded by NSERC of Canada. M.G. acknowledges the Research Corporation for a Research Innovation Award and a Cottrell Scholar Award, and the Province of Ontario for a Premier Research Excellence Award.

-
- [1] For recent reviews see: A.P. Ramirez, *Annu. Rev. Mater. Sci.*, **24**, 453, (1994); *Magnetic Systems with Competing Interactions*, edited by H.T. Diep (World Scientific, Singapore, 1994); P. Schiffer and A.P. Ramirez, *Comm. Cond. Mat. Phys.*, **18**, 21, (1996); M.J.P. Gingras, to appear in *J. Phys. Cond. Matt.* A.P. Ramirez, to appear in *Handbook of Magnetic Materials*.
 - [2] P. Chandra and P. Coleman, *New Outlooks and Old Dreams in Quantum Antiferromagnets*, Les Houches Summer School Lectures, North Holland, Amsterdam; Eds. Douçot and Zinn-Justin, 1991.
 - [3] E.F. Shender and P.C.W. Holdsworth, in *Fluctuations And Order: A New Synthesis*, Ed. M.M. Millonas, Springer-Verlag, 1996.
 - [4] C.L. Henley, cond-mat/0009130.

- [5] R. Moessner, cond-mat/0010301.
- [6] G. Toulouse, Commun. Phys. **2**, 115 (1977).
- [7] G.H. Wannier, Phys. Rev. **79**, 357 (1950).
- [8] C.L. Henley, J. App. Phys. **61**, 3962 (1987).
- [9] W. Minor and T.M. Giebultowicz, J. Phys. (Paris), Colloq. **49**, C8-1551 (1988); H.T. Diep and H. Kawamura, Phys. Rev. B **40**, 7019 (1989).
- [10] B.E. Larson and C.L. Henley, (“Ground State Selection in Type III FCC Vector Antiferromagnets”), unpublished.
- [11] M. T. Heinila and A. S. Oja, Phys. Rev. B, **48**, 16514 (1993) and references therein.
- [12] P. Hakonen, O.V. Lounasmaa, and A. Oja, J. Mag. Magn. Mater. **100**, 394 (1991).
- [13] C. Wengel, C.L. Henley, and A. Zippelius, Phys. Rev. B **53**, 6543 (1995).
- [14] E.F. Shender, Sov. Phys. JETP, **56**, 178 (1982).
- [15] C.L. Henley, Phys. Rev. Lett. **62**, 2056 (1989).
- [16] J.N. Reimers, J.E. Greedan, and M. Björgvinsson, Phys. Rev. B **45**, 7295 (1992).
- [17] J.A. Mailhot and M.L. Plumer, Phys. Rev. B **48**, 9881 (1993).
- [18] S.T. Bramwell, M.J.P. Gingras and J.N. Reimers, J. Appl. Phys. **75**, 5523 (1994).
- [19] Random disorder can also cause a ground state selection. L. Bellier-Castella, M.J.P. Gingras, P.C.W. Holdsworth, R. Moessner, cond-mat/0006306. See also Ref. [4] and references therein.
- [20] A.B. Harris, C. Kallin and A.J. Berlinsky, Phys. Rev. B, **45**, 2899 (1992).
- [21] J.N. Reimers, A.J. Berlinsky, and A.-C. Shi, Phys. Rev. B **43**, 865 (1991).
- [22] N.P. Raju, M. Dion, M. J. P. Gingras, T.E. Mason and J.E. Greedan, Phys. Rev. B **59**, 14489 (1999)
- [23] S. E. Palmer and J. T. Chalker Phys. Rev. B **62**, 488 (2000); S.E. Palmer, Ph.D. thesis, Univ. of Oxford (October 2000).
- [24] S.T. Bramwell, *Crystal and Magnetic Structure of Isotopic Gadolinium Titanate*, ISIS Experimental Report, Rutherford Appleton Laboratory. ISIS99 report #10394, (<http://www.isis.rl.ac.uk>).
- [25] M.J. Harris, S. T. Bramwell, D. F. McMorrow, T. Zeiske, and K. W. Godfrey, Phys. Rev. Lett **79**, 2554 (1997).
- [26] S.T. Bramwell and M.J. Harris, Phys. Condens. Matt. **10**, L215 (1998).
- [27] The statistical mechanics problem with local ferromagnetically coupled (111) Ising spins maps onto a problem of antiferromagnetically coupled Ising spins residing on the pyrochlore lattice but now pointing along the global $\pm z$ direction. See Ref. [28].
- [28] P.W. Anderson, Phys. Rev. **102**, 1008 (1956).
- [29] D. Bernal and R. H. Fowler, J. Chem. Phys. **1**, 515 (1933).
- [30] L. Pauling, *The Nature of the Chemical Bond*, (Cornell Univ. Press, Ithaca, New York, 1945).
- [31] A. P. Ramirez, A. Hayashi, R.J. Cava, R. Siddharthan and B.S. Shastry, Nature **399**, 333 (1999).
- [32] R. Siddharthan, B. S. Shastry, A. P. Ramirez, A. Hayashi, R. J. Cava, S. Rosenkranz, Phys. Rev. Lett. **83**, 1854 (1999).
- [33] S. Rosenkranz, A.P. Ramirez, A. Hayashi, R.J. Cava, R. Siddharthan, B.S. Shastry, J. Appl. Phys. **87**, 5914 (2000).
- [34] S.T. Bramwell, J.S. Gardner, B.C. den Hertog, M.J.P. Gingras, A.L. Cornelius, M.J. Harris, D.F. McMorrow, A.R. Wildes, J.D.M. Champion, R.G. Melko and T. Fennell, unpublished (2000).
- [35] J.S. Gardner, S.R. Dunsiger, B.D. Gaulin, M.J.P. Gingras, J.E. Greedan, R.F. Kiefl, M.D. Lumsden, W.A. MacFarlane, N.P. Raju, J.E. Sonier, I. Swainson and Z. Tun, Phys. Rev. Lett. **82**, 1012 (1999).
- [36] M. J. P. Gingras, B. C. den Hertog, M. Faucher, J.S. Gardner, L.J. Chang, N.P. Raju, B.D. Gaulin, and J.E. Greedan, Phys. Rev. B **61**, 6496 (2000).
- [37] M. Kanada, Y. Yasui, Masanori Ito, H. Harashina1, M. Sato, H. Okumura and K. Kakurai, J. Phys. Soc. Japan, **68**, 3802 (1999).
- [38] $Tb_2Ti_2O_7$ is a more complicated case than $Dy_2Ti_2O_7$ and $Ho_2Ti_2O_7$. This system is not a perfect (111) Ising model since $\theta_{CW} \sim -20$ is not small compared to the low-lying single ion crystal electric field levels at energies of ~ 20 K and ~ 100 K above the ground state Ising doublet [35,36].
- [39] M.J. Harris, S.T. Bramwell, P.C.W. Holdsworth, and J.D.M. Champion, Phys. Rev. Lett. **81**, 4496 (1998).
- [40] R. Moessner, Phys. Rev. B **57**, R5587 (1998).
- [41] B.C. den Hertog and M.J.P. Gingras, Phys. Rev. Lett. **84**, 3430 (2000).
- [42] B.C. den Hertog, R.G. Melko, and M.J.P. Gingras, cond-mat/0009225.
- [43] J.E. Greedan, N.P. Raju, A.S. Wills, C. Morin, S.M. Shaw, and J.N. Reimers, Chem. Materials **10**, 3058 (1998).
- [44] R. Siddharthan, B. S. Shastry, A. P. Ramirez, cond-mat/0009265.
- [45] The Monte Carlo simulation was carried out on an $L = 6$ cubic system of 3456 spins. The system was cooled slowly down to $T=0.75$ K in the paramagnetic phase, which is slightly above the T_f value reported in Ref. [32]. The spin correlations due to paramagnetic fluctuations at this temperature were measured every 200 Monte Carlo MC steps over a total simulation length of 10^5 Monte Carlo steps per spin with a 12% acceptance rate. We used the following expression for the neutron scattered intensity, $I(\mathbf{q})$:
- $$I(\mathbf{q}) \propto |f(q)|^2 \frac{1}{N} \sum_{ij} e^{i\mathbf{q}\cdot(\mathbf{r}_i-\mathbf{r}_j)} \langle \mathbf{S}_{i,\perp}^{z_i} \cdot \mathbf{S}_{j,\perp}^{z_j} \rangle$$
- where $z_i = (1, 1, 1)$, $\langle \dots \rangle$ denotes a thermal average and $\mathbf{S}_{i,\perp}^{z_i}$ is the spin component at site i perpendicular to \mathbf{q} . The form factor $f(q)$ for Ho^{3+} was calculated in the small- \mathbf{q} approximation. Strong intensity due to the onset of short range correlations was observed at the exact wavelengths suggested by our mean field analysis with a cut off at the 5th nearest neighbour.
- [46] P. Gupta, S. Teitel, and M.J.P. Gingras, Phys. Rev. Lett. **80**, 105 (1997) and references therein.
- [47] C. Denniston and C. Tang, Phys. Rev. B **60**, 3163 (1999).
- [48] E.H. Lieb, Phys. Rev. Lett. **18**, 1046 (1967); *ibid.* **19**, 108 (1967).
- [49] M.E.J. Newman and G.T. Barkema, *Monte Carlo Methods in Statistical Physics*, (Clarendon Press, Oxford,1999). E.H. Lieb and F.Y. Wu, *Phase Transitions and Critical Phenomena, vol 1*, edited by C. Domb and J.L. Lebowitz, (Academic Press, London, 1970).